BRIEF COMMUNICATION

Crystal Structure and Magnetic Properties of $(Ni_{6-x}Cu_x)MnO_8$

Hideki Taguchi,[1] Akiko Ohta, and Mahiko Nagao

Research Laboratory for Surface Science, Okayama University, Okayama 700, Japan

and

Hiroyasu Kido

Osaka Municipal Technical Institute, Morinomiya, Jyoto-ku, Osaka 536, Japan

Murdochite-type $(Ni_{6-x}Cu_x)MnO_8$ $(0.0 \leq x \leq 0.4)$ was synthesized at 873 K using the precursor method. Both the (Ni, Cu)–O(1) and Mn–O(1) distances increase slightly with increasing x. These increases depend on the difference between the ionic radii of the Ni^{2+} and the Cu^{2+} ions. The magnetic measurement indicates that the $1/\chi$–T curve has a step caused by the mixture of the antiferromagnetic cluster due to the 180° superexchange interaction for (Ni^{2+}, Cu^{2+})–O–(Ni^{2+}, Cu^{2+}) and the paramagnetic spins. © 1998 Academic Press

Murdochite-type Ni_6MnO_8 is considered to be derived from the rock-salt structure of NiO by the replacement of one-eighth of the Ni^{2+} ions with the Mn^{4+} ions and one-eighth with vacancies (1–3). The space group of Ni_6MnO_8 is reported to be $Fm3m$ (1). The Mn^{4+} ions and vacancies occupy (111) alternate lattice layers and are ordered within the layers. Both the Ni^{2+} and Mn^{4+} ions are octahedrally coordinated by six oxygen ions.

Murdochite-type $(Ni_{1-x}Mg_x)_6MnO_8$ is synthesized using the precursor method (4). The linear increase in the (Ni, Mg)–O and the Mn–O distances depends on the difference between the ionic radii of the Ni^{2+} and Mg^{2+} ions (5). From the magnetic measurement, the $1/\chi$–T curve displays a step that corresponds to the Néel temperature (T_N). Although the ionic radius of the Cu^{2+} ion is nearly equal to that of the Mg^{2+} ion (5), the Cu^{2+} ion has nine 3d electrons. Therefore, it is assumed that the magnetic properties of murdochite-type $(Ni_{6-x}Cu_x)MnO_8$ are strongly influenced by the Cu^{2+} ion. In the present study, we synthesized $(Ni_{6-x}Cu_x)MnO_8$ and refined the crystal structure by Rietveld analysis. The

magnetic susceptibility was measured to make clear the superexchange interactions for (Ni^{2+}, Cu^{2+})–O–(Ni^{2+}, Cu^{2+}) and (Ni^{2+}, Cu^{2+})–O–Mn^{4+}.

$(Ni_{6-x}Cu_x)MnO_8$ was prepared using the precursor method (1, 4). The powders (3.000 g) of $Ni(CH_3COOH)_2 \cdot 4H_2O$, $Cu(CH_3COOH)_2 \cdot H_2O$, and $Mn(CH_3COOH)_2 \cdot 4H_2O$ were weighted in the appropriate proportions and dissolved in 100 cm³ of 0.25 M acetic acid. Then, the 0.30 M aqueous solution (100 cm³) of oxalic acid was added. The resulting solution was mixed and evaporated to dryness in a rotary evaporator at 323–343 K. The obtained powder was fired in air at 873 K for 3 h. The heating rate was 3 K/min. The phases of the samples were identified by X-ray diffraction (XRD) with monochromatic Cu$K\alpha$ radiation. XRD data was collected by step scanning over an angular range $15° \leq 2\theta \leq 95°$ in increments of 0.02° (2θ). The structure refinement was carried out by Rietveld analysis of the XRD data with the "RIETAN" program written by Izumi (6). The magnetic susceptibility of the samples was measured by a magnetic torsion balance.

XRD patterns of $(Ni_{6-x}Cu_x)MnO_8$ $(0.0 \leq x \leq 0.4)$ were completely indexed as the murdochite-type structure. On refining the crystal structure, isotropic thermal parameters (B) for the Ni, Cu, Mn, O(1), and O(2) atoms were refined assuming that they had the same values. Refined structure parameters and residuals, weighted pattern R factor (R_{WP}), pattern R factor (R_P), integrated R factor (R_I), and structure factor (R_F) are listed in Table 1. The final R_F of all samples were less than 2.75%, and low R_F suggests that the structure model for $(Ni_{6-x}Cu_x)MnO_8$ is reasonable.

The ionic radii of the Ni^{2+} and the Cu^{2+} ions with a coordination number (CN) of 6 are 0.070 and 0.073 nm, respectively (5). Therefore, the slight increase in the cell constant is explained by the difference between the ionic

---

[1] To whom correspondence should be addressed.

TABLE 1
Refined Structure Parameters for $(Ni_{6-x}Cu_x)MnO_8$

Atom	Position	x	y	z
$x = 0$	$a = 0.83200(2)$ nm		$B = 0.002(2)$ nm^2	
$R_{WP} = 10.77\%$	$R_P = 7.53\%$	$R_I = 3.11\%$	$R_F = 2.32\%$	
Ni, Cu	24(d)	0	0.25	0.25
Mn	4(a)	0	0	0
O(1)	8(c)	0.25	0.25	0.25
O(2)	24(e)	0.231(2)	0	0
$x = 0.1$	$a = 0.83204(2)$ nm		$B = 0.003(1)$ nm^2	
$R_{WP} = 9.58\%$	$R_P = 6.77\%$	$R_I = 2.57\%$	$R_F = 2.18\%$	
Ni, Cu	24(d)	0	0.25	0.25
Mn	4(a)	0	0	0
O(1)	8(c)	0.25	0.25	0.25
O(2)	24(e)	0.230(2)	0	0
$x = 0.2$	$a = 0.83211(2)$ nm		$B = 0.003(1)$ nm^2	
$R_{WP} = 8.92\%$	$R_P = 6.45\%$	$R_I = 2.40\%$	$R_F = 2.01\%$	
Ni, Cu	24(d)	0	0.25	0.25
Mn	4(a)	0	0	0
O(1)	8(c)	0.25	0.25	0.25
O(2)	24(e)	0.230(2)	0	0
$x = 0.3$	$a = 0.83234(2)$ nm		$B = 0.003(1)$ nm^2	
$R_{WP} = 8.76\%$	$R_P = 6.28\%$	$R_I = 2.44\%$	$R_F = 2.13\%$	
Ni, Cu	24(d)	0	0.25	0.25
Mn	4(a)	0	0	0
O(1)	8(c)	0.25	0.25	0.25
O(2)	24(e)	0.230(2)	0	0
$x = 0.4$	$a = 0.83255(2)$ nm		$B = 0.003(2)$ nm^2	
$R_{WP} = 9.31\%$	$R_P = 6.63\%$	$R_I = 2.86\%$	$R_F = 2.75\%$	
Ni, Cu	24(d)	0	0.25	0.25
Mn	4(a)	0	0	0
O(1)	8(c)	0.25	0.25	0.25
O(2)	24(e)	0.231(2)	0	0

TABLE 2
(Ni, Cu)−O and Mn−O Distances (nm) for $(Ni_{6-x}Cu_x)MnO_8$

x	(Ni, Cu)−O(1)	(Ni, Cu)−O(2)	Mn−O(1)	Mn−O(2)
0	0.20800(1)	0.20860(12)	0.20800(1)	0.1923(16)
0.1	0.20801(1)	0.20867(11)	0.20801(1)	0.1915(14)
0.2	0.20803(1)	0.20871(11)	0.20803(1)	0.1912(13)
0.3	0.20809(1)	0.20875(12)	0.20809(1)	0.1914(15)
0.4	0.20814(1)	0.20871(13)	0.20814(1)	0.1926(18)

the composition (x). The broken line indicates the theoretical μ_{eff} that was calculated on the assumption of the Ni^{2+} ions with the $(d\varepsilon)^6(d\gamma)^2$, the Cu^{2+} ions with the $(d\varepsilon)^6(d\gamma)^3$, and the Mn^{4+} ions with the $(d\varepsilon)^3(d\gamma)^0$. The observed μ_{eff} is larger by $\approx 2\mu_B$ than the theoretical μ_{eff} in the range $0.0 \leq x \leq 0.1$, while the observed μ_{eff} is close to the theoretical μ_{eff} in the range $0.1 \leq x \leq 0.4$. We could observe the same variation in $(Ni_{1-x}Mg_x)_6MnO_8$. Since the Ni^{2+} ion content is 5.6–6.0 times the Mn^{4+} ion content, it is assumed that the (Ni, Cu)O$_6$ octahedron dominates the magnetic property. In the Ni^{2+} ion-rich region, the (Ni, Cu, or Mg)−O(2) distance is nearly equal to the Ni−O distance (≈ 0.2089 nm) for NiO (8), while the (Ni, Cu, or Mg)−O(1) distance is shorter than the Ni−O distance for NiO. The (Ni, Cu, or Mg)−O(1) distance increases with increasing x, and the increase in the (Ni, Cu, or Mg)−O(1) distance makes the distortion of the (Ni, Cu, or Mg)O$_6$ octahedra cancel. Consequently, it is considered that the observed μ_{eff} is close to the theoretical μ_{eff}.

The magnetic properties of $(Ni_{6-x}Cu_x)MnO_8$ depend on the 180° superexchange interactions for (Ni^{2+}, Cu^{2+})−O−(Ni^{2+}, Cu^{2+}) and the 90° superexchange interactions for (Ni^{2+}, Cu^{2+})−O−(Ni^{2+}, Cu^{2+}) and (Ni^{2+}, Cu^{2+})−O−Mn^{4+}. In the murdochite-type structure, there are no 180° superexchange interactions for (Ni^{2+}, Cu^{2+})−O−Mn^{4+} and

radii of the Ni^{2+} and the Cu^{2+} ions. Both the (Ni, Cu)−O and Mn−O distances increase slightly as shown in Table 2. The difference between the (Ni, Cu)−O(1) and the (Ni, Cu)−O(2) distances is $\approx 0.3\%$, while the difference between the Mn−O(1) and the Mn−O(2) distances is $\approx 7.8\%$. There is the same tendency for the Ni^{2+} ion-rich region in $(Ni_{1-x}Mg_x)_6MnO_8$. From these results, it is considered that the MnO$_6$ octahedron has a large distortion in comparison with the (Ni, Cu)O$_6$ octahedron.

Figure 1 shows the relationship between the inverse magnetic susceptibility ($1/\chi$) and temperature. The steps were observed in the $1/\chi–T$ curves and decrease slightly with increasing x; ≈ 455 K for $x = 0.0$, ≈ 453 K for $x = 0.1$, ≈ 451 K for $x = 0.2$, ≈ 449 K for $x = 0.3$, and ≈ 448 K for $x = 0.4$, respectively. It is considered that the step is caused in the same way as $(Ni_{1-x}Mg_x)_6MnO_8$; that is, the step is due to the mixture of the antiferromagnetic cluster and paramagnetic spins (4, 7). Figure 2 shows the relationship between the observed effective magnetic moment (μ_{eff}) and
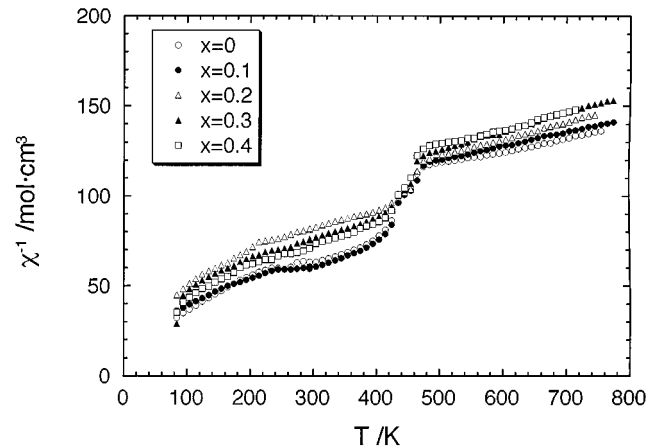

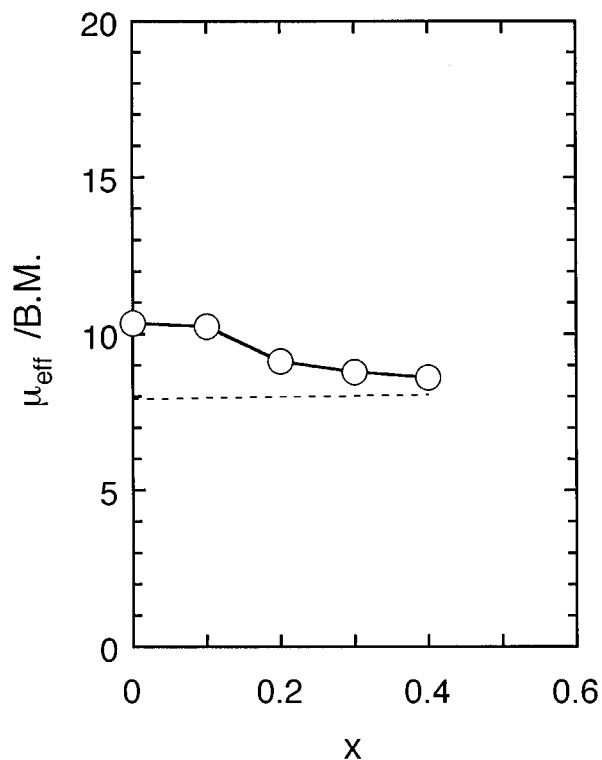**FIG. 1.** Inverse magnetic susceptibility ($1/\chi$) vs temperature (T) for $(Ni_{6-x}Cu_x)MnO_8$.

FIG. 2. The effective magnetic moment (μ_{eff}) vs composition (x) for $(Ni_{6-x}Cu_x)MnO_8$. Broken line indicates the theoretical μ_{eff}.

Mn^{4+}–O–Mn^{4+} or the 90° superexchange interaction for Mn^{4+}–O–Mn^{4+}. The 180° superexchange interaction for Ni^{2+}–O–Ni^{2+} is antiferromagnetic (9). The variation of T_N for rock-salt type $(Ni_{1-x}Cu_x)O$ indicates that the 180° superexchange interaction for (Ni^{2+}, Cu^{2+})–O–(Ni^{2+}, Cu^{2+}) is antiferromagnetic and decreases with increasing x (10). The 90° superexchange interactions for Ni^{2+}–O–

Ni^{2+} and Ni^{2+}–O–Mn^{4+} are antiferromagnetic and ferromagnetic, respectively (11). Although we have no information about the 90° superexchange interactions for (Ni^{2+}, Cu^{2+})–O–(Ni^{2+}, Cu^{2+}) and (Ni^{2+}, Cu^{2+})–O–Mn^{4+}, it is considered that the 180° superexchange interactions for (Ni^{2+}, Cu^{2+})–O–(Ni^{2+}, Cu^{2+}) is dominant in the magnetic properties of $(Ni_{6-x}Cu_x)MnO_8$. Since the Mg^{2+} ion has no $3d$ electrons, it is obvious that the 180° superexchange interaction for (Ni^{2+}, Mg^{2+})–O–(Ni^{2+}, Mg^{2+}) decreases abruptly with increasing x. On the other hand, the 180° superexchange interaction for (Ni^{2+}, Cu^{2+})–O–(Ni^{2+}, Cu^{2+}) decreases slightly with increasing x. Therefore, the variation of the step for $(Ni_{6-x}Cu_x)MnO_8$ is different from that for $(Ni_{1-x}Mg_x)_6MnO_8$.

REFERENCES

1. P. Porta, G. Minelli, I. L. Botto, and E. J. Baran, *J. Solid State Chem.* **92,** 202 (1991)
2. J. S. Kasper and J. S. Prener, *Acta. Crystallogr.* **7,** 246 (1954).
3. P. Porta and M. Valigi, *J. Solid State Chem.* **6,** 344 (1973).
4. H. Taguchi, S. Omori, M. Nagao, H. Kido, and M. Shimada, *J. Solid State Chem.* **118,** 112 (1995).
5. R. D. Shannon and R. D. Prewitt, *Acta Crystallogr. B* **25,** 925 (1969).
6. F. Izumi, in "The Rietveld Method," (R. A. Young, Ed.), Chap. 13, Oxford University Press, Oxford, 1993.
7. A. Z. Menshikov, Y. A. Dorofeev, A. G. Klimenko, and N. A. Mironova, *Phys. Status Solidi (b)* **164,** 275 (1991).
8. J. C. P. D. S. 4-0835.
9. J. B. Goodenough, "Magnetism and the Chemical Bond," p. 190, Wiley, New York, 1963.
10. P. Grange, H. Charcosset, P. Gallezot, P. Turlier, and J. Vialle, *J. Solid State Chem.* **11,** 26 (1974).
11. J. Kanamori, *J. Phys. Chem. Solids* **10,** 87 (1959).
12. S. P. Kowalczyk, L. Ley, F. R. McFeely, and D. A. Shirley, *Phys. Rev., B* **11,** 1721 (1975).